OPTIMAL RECEIVER CONFIGURATION OF SHORT-BASELINE LOCALISATION SYSTEMS USING PARTICLE SWARM OPTIMISATION

Christoph Tholen, Tarek El-Mihoub,
Lars Nolle, Oliver Ralle
Autonomous Systems Research Group
Department of Engineering Science
Jade University of Applied Sciences
Email: {christoph.tholen | tarek.el-mihoub |
lars.nolle }@jade-hs.de
oliver.ralle@student.jade-hs.de

Robin Rofallski
Institute for Applied Photogrammetry and
Geoinformatics
Jade University
of Applied Sciences
Oldenburg, Germany
robin.rofallski@jade-hs.de

KEYWORDS
SBL, AUV, Optimisation, Short-Baseline-Localisation, Underwater Acoustic Localisation, Autonomous-Underwater-Vehicles

ABSTRACT

This work investigates the localisation error of a short-baseline system used for the localisation of submerged underwater vehicles. In a first step, different possible error influences are identified and their numerical simulation are described. In a second step, this simulation is used to determine the optimal position of the acoustic receivers of the system using Particle Swarm Optimisation and Monte-Carlo simulations. The positioning error of the optimised receiver arrangement is 6.64 % smaller than the error of a standard arrangement.

INTRODUCTION

The use of autonomous underwater vehicles (AUVs) requires a method for robust, reliable and accurate determination of an AUV's position. Autonomous vehicle usually rely on the availability of global navigation satellite systems (GNSS) in order to estimate their global position. However, the electromagnetic signals of such satellite systems cannot be received by submerged AUVs (Wu, et al., 2019). Different possible methods for localisation of submerged AUVs were proposed in the past. These methods can be classified into inertial or dead reckoning, acoustic methods and geophysical methods (Paull, et al., 2014). This paper focusses on the accuracy of an acoustic based localisation method called short-baseline localisation (SBL) (Paull, et al., 2014). The system under investigation is an off-the-shelf low-cost positioning system (Water Linked AS, 2020). In this work, different error sources, decreasing the accuracy of an acoustic based localisation system, are investigated. In order to increase the localisation accuracy of the system, the optimal receiver configuration is determined using Monte Carlo simulations and Particle Swarm Optimisation.

SHORT-BASELINE-LOCALISATION

Acoustic based localisation methods, like SBL, use the time of flight principle of acoustic waves (Paull, et al., 2014). The system usually consists of a couple of transducers, mounted on a mothership or a jetty and a single receiver mounted on an AUV (Figure 1). The transducers are emitting acoustic signals. The time of flight (TOF), i.e. the time between the emission and the reception of the signals, is measured by the receiver mounted on the AUV. Subsequently, the TOF can be used to calculate the position of the AUV.

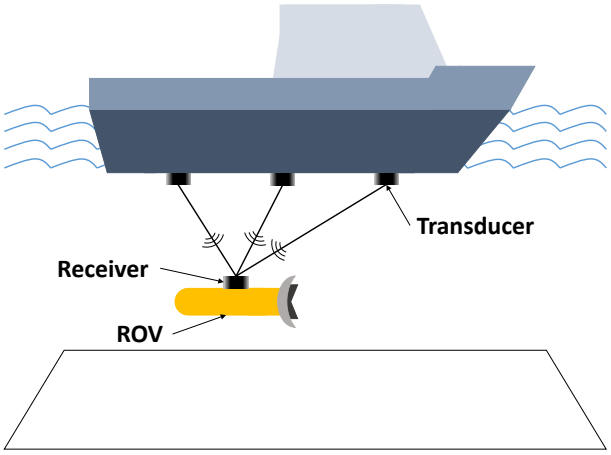

Figure 1: Principle of Short-Baseline localisation methods modified after (Wu, et al., 2019)

However, the Water Linked system used in this research uses a single transducer, or locator, mounted on the AUV and four receivers mounted on a mothership or a jetty (Water Linked AS, 2020). The locator emits an acoustic signal, which is received by the four receivers. The time between the emission and the reception of the signal is measured individually by the four receivers. The principle of the Water Linked SBL system is shown in Figure 2.

Communications of the ECMS, Volume 34, Issue 1,
Proceedings, ©ECMS Mike Steglich, Christian Mueller,
Gaby Neumann, Mathias Walther (Editors)
ISBN: 978-3-937436-68-5/978-3-937436-69-2(CD) ISSN 2522-2414

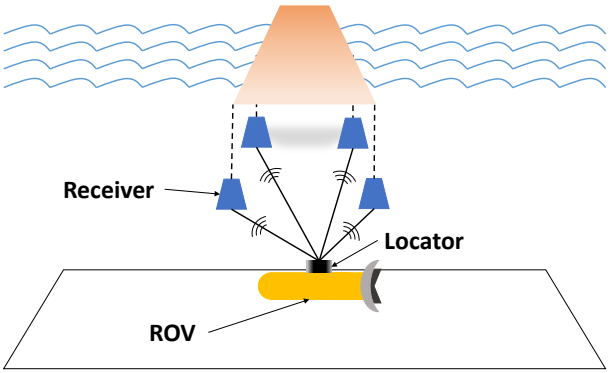

Figure 2: Water Linked SBL System

To localise an AUV using an SBL system usually a spherical-based algorithm is used (Turetta, et al., 2014). It uses the distances between the AUV and the SBL receivers to estimate the AUV's position. The distances d_i are determined by measuring the time of flight t_i for each receiver. Given the speed of sound v, the distances d_i for n receivers are calculated as follows:

$$d_i = t_i \cdot v \tag{1}$$

Where:
d_i : Distance between receiver i and AUV,
t_i : Time of flight measured by receiver i,
v : Speed of sound.

In a Cartesian coordinate system, the Euclidean distances d_i can be decomposed into the x, y, and z components as follows:

$$(x - x_i)^2 + (y - y_i)^2 + (z - z_i)^2 = d_i^2 \tag{2}$$

Where:
$[x,y,z]$: Coordinates of the AUV,
$[x_i,y_i,z_i]$: Coordinates of the receiver i.

The z-coordinate of the AUV usually is determined using an on-board pressure sensor (Turetta, et al., 2014). Thus, the 3D problem can be reduced to a 2D problem in the x-y-plane with the planar distances r_i between the AUV and the receiver i:

$$r_i^2 = d_i^2 - (z - z_i)^2 \tag{3}$$

From equations (2) and (3) follows:

$$(x - x_i)^2 + (y - y_i)^2 = r_i^2 \tag{4}$$

Equation (4) leads to the linear relationship with four receivers and the position vector $X = [x, y]^T$:

$$A \cdot X = R - D \tag{5}$$

With:

$$A = \begin{bmatrix} x_1 - x_2 & y_1 - y_2 \\ x_2 - x_3 & y_2 - y_3 \\ x_3 - x_4 & y_3 - y_4 \\ x_4 - x_1 & y_4 - y_1 \end{bmatrix},$$

$$R = \frac{1}{2}\begin{bmatrix} r_2^2 - r_1^2 \\ r_3^2 - r_2^2 \\ r_4^2 - r_3^2 \\ r_1^2 - r_4^2 \end{bmatrix},$$

$$D = \frac{1}{2}\begin{bmatrix} (x_2^2 + y_2^2) - (x_1^2 + y_1^2) \\ (x_3^2 + y_3^2) - (x_2^2 + y_2^2) \\ (x_4^2 + y_4^2) - (x_3^2 + y_3^2) \\ (x_1^2 + y_1^2) - (x_4^2 + y_4^2) \end{bmatrix}.$$

By using the least squares method, the position of the AUV can be estimated as follows (Turetta, et al., 2014):

$$\hat{X} = (A^T \cdot A)^{-1} \cdot A^T \cdot (R - D) \tag{6}$$

With:

$$\hat{X} = [\hat{x}, \hat{y}]^T .$$

In the absence of measurement errors, the described spherical-based algorithm guarantees an accurate estimation of the actual AUV position. However, in a real world application, measurement errors affect the accuracy of the SBL system. The accuracy of an acoustic positioning system can be determined using experiments (Almeida, et al., 2016) or numerical simulations (Turetta, et al., 2014). In the next chapter, different error sources and their impact on the localisation process are described.

ERROR FORMULATION

From equations (1) to (3), the following potential sources of error are identified: determination of the receivers' positions, accuracy of the measurements of TOF, determination of the speed of sound and accurate calculation of the actual depth of the AUV. These potential sources of error are discussed in more detail below.

Receiver Position

Usually, the position of the receivers is obtained using different measurement methods, like GPS (Almeida, et al., 2016), tape measurements or using a total station. The accuracy of the measurements depend on the chosen method. It ranges from millimetre to decimetre accuracy. During operation, the receivers might be affected by currents and waves, resulting in periodical drift of the receivers.
In this work tape measuring is simulated. Therefore, both effects are modelled using a truncated Gaussian distribution with the maximum value of $x_{max} = 0.02$ m, the true locator position as mean value and a standard deviation of $\sigma_{xy} = 0.05$ m for the x and y position of the receivers. The error of the z position is modelled using a Gaussian distribution with the true position as mean value and a standard deviation of $\sigma_z = 0.05$ m.

Time of Flight

The TOF measurements are affected if the clocks used in the locator and in the receiver are not synchronised

(Paull, et al., 2014). Also, a quantisation error is introduced by the signal-processing unit (Turetta, et al., 2014).
The Water Linked system, used in this work, utilises GPS time to avoid these synchronisation issues (Water Linked AS, 2020). Based on the specifications of the system used, the TOF error is simulated using a Gaussian distribution with the true time of flight as mean value and a standard deviation of $\sigma_{ToF} = 10^{-6}$s.

Speed of Sound

The speed of sound in seawater depends on temperature, salinity and pressure of the seawater (UNESCO, 1983). In the water column, temperature and salinity vary over time (Tholen, et al., 2020). Hence, the speed of sound also varies. For the accurate determination of the speed of sound, the path d_i of the sound wave from the locator to receiver i has to be taken into account:

$$v_i = \frac{1}{d_i}\int_0^{d_i} v(S(d), T(d), P(d))\, dd \tag{7}$$

Where:
d_i : Path from transducer to the receiver i,
$S(d)$: Salinity as function of the path,
$T(d)$: Temperature as function of the path,
$P(d)$: Pressure as function of the path.

The calculation of the speed of sound using (7) requires detailed knowledge about the temperature and salinity distribution within the area under investigation. However, for this work, the knowledge is actually not available. Therefore, the speed of sound is calculated using the UNESCO formula (UNESCO, 1983) with a fixed value for the temperature, the salinity and the pressure. The values of the environmental parameters are randomly selected from a Gaussian distribution. The mean values and the standard deviation are calculated from data recorded during a test dive in a harbour in Fremantle, Western Australia. The mean values and the standard deviations of the environmental parameters are summarised in Table 1.

Table 1: Environmental Parameters simulated

Parameter	$\bar{x}$	σ
Temperature	22.54 °C	0.054 °C
Salinity	23.35 PSU	0.675 PSU
Pressure	1086.1 mbar	28.41 mbar

AUV Depth

Usually, the actual depth of an AUV is calculated using an on-board pressure sensor. The pressure measured by the sensor is the sum of the barometric pressure P_{amb} and the hydrostatic pressure P_{hyd} caused by the water column above the sensor. Due to the slow change rate and the small variation of the barometric pressure, compared to the hydrostatic pressure, changes of the barometric pressure are neglected in this paper.

The hydrodynamic pressure is affected by the density of the seawater $\rho_{seawater}$, the gravity acceleration g and, the height of the water column z. The density of seawater is a function of temperature, salinity and pressure (UNESCO, 1983). The pressure dependency can be neglected if the maximum depth is less than 100 m (Nayar, et al., 2016). The temperature and salinity vary within the depth. The pressure at depth z can be calculated as follows:

$$P = g \cdot \int_0^z \rho\big(S(z), T(z)\big)\, dz \tag{8}$$

Where:
g : gravity acceleration,
$S(z)$: Salinity as function of the depth z,
$T(z)$: Temperature as function of the depth z,
$\rho()$: Density as function of salinity and temperature,
z : Depth.

The calculation of the pressure using (8) requires detailed knowledge about the temperature and salinity distribution. However, for this work, this information is not available. Therefore, the speed of sound is calculated using a Gaussian distribution of the temperature and salinity (Table 1). In the simulations presented in this work, the pressure is calculated as follows:

$$P = g \cdot \rho(\bar{T}, \bar{S}) \cdot z \tag{9}$$

Where:
g : gravity acceleration,
$\rho(\bar{T}, \bar{S})$: Density as function of average temperature and salinity,
z : Depth.

The calculated pressure value is measured by the on-board pressure sensor of the ROV. The pressure reading of the sensor is affected by measurement errors. This measurement error is modelled using a Gaussian distribution with the actual value of P as mean value and a standard deviation of $\sigma_{Pressure\ Sensor} = 40\ Pa$. This pressure is used to calculate the estimated depth $\tilde{z}$ of the ROV. In addition, the ROV measures the temperature and the salinity in order to estimate the speed of sound and the density. The measurement errors are modelled using a Gaussian distribution with the real values as mean values and standard deviations based on the sensor specifications. The standard deviation of the temperature sensor was set to $\sigma_{Temperature\ Sensor} = 0.05\ °C$ and the standard deviation of the salinity sensor was set to $\sigma_{Salinity\ Sensor} = 0.84\ PSU$.

SIMULATIONS

As shown in the previous section, different parameters, like the speed of sound or the movement of the receivers, have an influence on the performance of an acoustic based localisation system. In addition, the chosen baseline, i.e. the distance between the receivers, has an influence on the performance of the SBL system (Paull,

et al., 2014). The error of an acoustic based localisation system depends on the distance between the transducer and the receiver (Turetta, et al., 2014) and, if the baseline is not symmetric, the position of the ROV with respect to the position of the baseline. Hence, n=100 positions within the search radius of 100 m were selected randomly. The points are selected once and used for all simulations, in order to allow a fair comparison between the different solutions.
All error sources described above are modelled using normal distributed random numbers. Hence, the localisation error depends on the random number generation. Therefore, for each chosen ROV position m=100 position evaluations are carried out following the algorithm presented in Figure 3. Here, variables marked with an asterisk represent true values, whereas variables marked with a tilde represent error affected values.

```
function compute estimated position:
  calculate T*(T̄, σ_T)     %real temperature
  calculate S*(S̄, σ_S)     %real salinity
  calculate v*(T*, S*)     %real speed of sound
  calculate ρ*(T*, S*)     %real density
  calculate t_i*(x_i*, x*, v*) %real time of flight (ToF)
  measure   t̃_i(t_i*, σ_t)     %ToF error affected (EA)
  calculate P*(ρ*, z)      %real pressure at depth z (Eq. 9)
  measure   P̃(P*, σ_P)     %pressure (EA)
  measure   T̃(T*, σ_T)     %temperature (EA)
  measure   S̃(S*, σ_S)     %salinity (EA)
  calculate ρ̃(T̃, S̃)       %density (EA)
  calculate z̃(ρ̃, P̃)       %depth of the ROV(EA)
  calculate ṽ(T̃, S̃)       %speed of sound (EA)
  calculate d̃_i(t̃_i, ṽ)    %distance ROV and receivers (EA)
  calculate x̃_i(x_i*, σ_x, max_x)%position of the receivers (EA)
  calculate r̃_i(d̃_i, x̃_i, z̃)  %planar radius (EA) (Eq.3)
  calculatex̂(r̃_i, x̃_i)     %estimated position (Eq. 5&6)
return x̂
```

Figure 3: Pseudocode to compute the estimated position

The localisation error of an estimated position is calculated as the Euclidean distance between the estimated position $\hat{x}$ and the real position x of the ROV as follows:

$$\varepsilon_j = \sqrt{\left(x - \hat{x}_j\right)^2 - \left(y - \hat{y}_j\right)^2 - \left(z - \hat{z}_j\right)^2} \qquad (10)$$

Where:
ϵ_j : Error of the evaluation j,
x, y, z : Real position of the ROV,
$\hat{x}, \hat{y}, \hat{z}$: Estimated position of the ROV.

Equation 10 gives the error of a single position estimation. In order to evaluate the performance of a chosen locator configuration, a fitness function is needed. The chosen fitness function should consider the errors of all ROV positions and all evaluations equally. Therefore, the fitness value of a chosen receiver configuration is calculated as follows:

$$f = \frac{\sum_{i=1}^{n}\left(\frac{\sum_{j=1}^{m}\epsilon_j}{m}\right)}{n} \qquad (11)$$

Where:
f : Fitness value of the receiver configuration,
ϵ_j : Error of the evaluation j,
n : Number of target positions,
m : Number of evaluations.

Previous published work recommends to setup the baseline as long as possible (Bingham, 2009). Furthermore, during simulations, the receivers are usually positioned on a rectangular shaped baseline, in order to simplify the spherical-based algorithm (Turetta, et al., 2014). According to the length of the locator cables and the requirements of a rectangular shaped baseline, a common baseline, using the Waterlinked SBL system, is shown in Figure 4. It can be observed from the figure that the locators are positioned at different depths. This shall improve the performance of the localisation algorithm (Water Linked AS, 2020). The localisation error of this common receiver configuration is determined to be f_{common} = 1.5386 m. The error of the optimised locator configuration should be less than the error of this standard configuration.

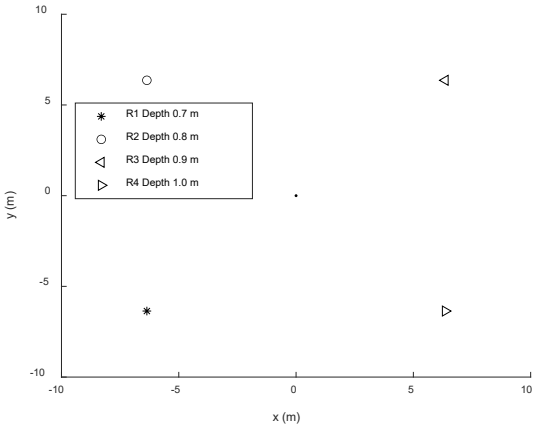

Figure 4: Common Baseline Configuration for the Waterlinked SBL

Since the length of the receiver cables is limited, the possible positions of the receivers are restricted. In addition, the cables should not be placed along the shortest possible routes, as there is a risk that propellers could damage the cables. The cables are placed in the x-y plane and then lowered to depth z. All receivers are connected to the main box of the SBL system, positioned at the origin of the coordinate system. Therefore, the cable length needed is calculated as follows:

$$d_i = \sqrt{x_i^2 + y_i^2} + z_i \qquad (12)$$

Where:
$[x_i, y_i, z_i]$: Coordinates of the receiver i.

All calculated cable length must be less than 10 m. Otherwise the cable length of the available receivers is not sufficient and the chosen receiver configuration cannot be used. In this case the fitness of this receiver

configuration will not be evaluated by using the simulation (Figure 3). Instead, a penalty value, bigger than the typical fitness values, is set as fitness value (Equation 13). This penalty strategy is commonly known as "death penalty" (Coello, 1999).

$$Penalty = \begin{cases} true; \ \max(d_i) > 10\ m \\ false; \ \max(d_i) \leq 10\ m \end{cases} \quad (13)$$

Where:

d_i : Euclidean distance between the receiver *i* and the origin of the SBL system.

PARTICLE SWARM OPTIMISATION

In this work, the optimal locator positions for the Water Linked SBL system are determined using particle swarm optimisation (PSO).

PSO is modelled on the behaviour of collaborative real world entities (particles), for example fish schools or flocks of birds, which work together to achieve a common goal (Kennedy & Eberhart, 1995). Each individual of the swarm searches for itself. However, the other swarm members also influence the search behaviour of each individual.

In the beginning of a search, each particle of the swarm starts at a random position and a randomly chosen velocity for each direction of the *n*-dimensional search space. Then, the particles move through the search space with an adjustable velocity. The velocity of a particle is based on its current fitness value, the best solution found so far by the particle (cognitive knowledge) and the best solution found so far by the whole swarm (social knowledge) (14):

$$\vec{v}_{i+1} = \vec{v}_i\omega + r_1c_1(\vec{p}_b - \vec{p}_i) + r_2c_2(\vec{g}_b - \vec{p}_i) \quad (14)$$

Where:

$\vec{v}_{i+1}$: new velocity of a particle,
$\vec{v}_i$: current velocity of a particle,
ω: inertia weight,
c_1: cognitive scaling factor,
c_2: social scaling factor,
r_1, r_2 : random number from range [0,1],
$\vec{p}_i$: current position of a particle,
$\vec{p}_b$: best known position of a particle,
$\vec{g}_b$: best known position of the swarm.

After calculating the new velocity of the particle, the new position $\vec{p}_{i+1}$ can be calculated as follows:

$$\vec{p}_{i+1} = \vec{p}_i + \vec{v}_{i+1}\Delta t \quad (15)$$

Where:

$\vec{p}_{i+1}$: new position of a particle,
$\vec{p}_i$: current position of a particle,
$\vec{v}_{i+1}$: new velocity of a particle,
Δt: time step (one unit).

In (15), Δt, which always has the constant value of one unit, is multiplied to the velocity vector $\vec{v}_{i+1}$ in order to receive consistency in the physical units (Nolle, 2015). In this research the control parameter values for all experiments were chosen as follows (Eberhardt & Shi, 2000):

ω = 0.1,
c_1 = 1.49,
c_2 = 1.49.

Figure 5 shows pseudocode of the optimisation framework described afore.

```
Init PSO
for each Iteration do:
  for each Particle do:
    choose Position of Locators
    calculate cable length (Eq. 12)
    check Penalty (Eq. 13)
    if Penalty is true do:
      set fitness value to 10
    else do:
      for each target-position do:
        for each evaluation do:
          compute estimated position (Fig. 3)
          calculate error (Eq. 10)
        end for
      end for
      calculate fitness value (Eq. 11)
    end if
    update pb and gb
    update v⃗ and p⃗
  end for
end for
```

Figure 5: Pseudocode for Optimisation of Locator Position

RESULTS

Seven experiments were carried out, which took approximately 30 hours on a high-end workstation. Figure 6 shows the development of the fitness values of the seven optimisation runs over time, i.e. iterations. It can be observed from the figure that, expect from one experiment, PSO was able to minimise the fitness of the given problem.

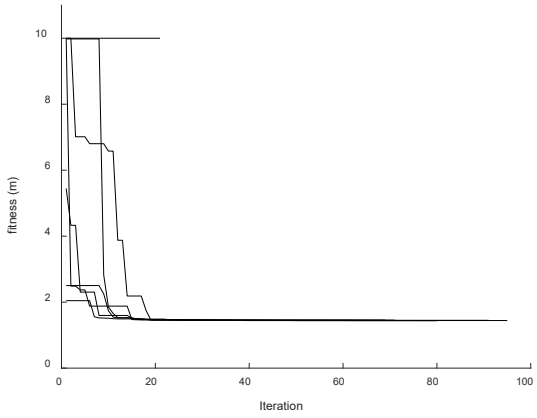

Figure 6: Fitness over Time for seven experiments

The g_b value of the different optimisation runs is given in Table 2. The mean fitness, except for run two, is $\bar{f}$ =

$1.4470\,m$ and the standard deviation of the fitness, except run two is $\sigma_f = 0.0072\,m$.

Table 2: g_{best} Values of the Optimisation runs

Run	g_{best}
1	1.4364
2	10
3	1.4540
4	1.4431
5	1.4496
6	1.4550
7	1.4441

The best receiver configuration was found in optimisation run one. The optimal position of the receivers is summarised in Table 3.

Table 3: Optimal Position of the Receivers

Receiver	x (m)	y (m)	z (m)
1	6.29	- 5.53	1.30
2	3.52	2.11	0.01
3	- 5.30	- 7.61	0.16
4	- 1.82	- 3.07	2.78

The optimal position of the four receivers is shown in Figure 7. It can be obtained from the figure, that, against the assumption, in the optimal configuration the receivers are not positioned in a rectangular shape.

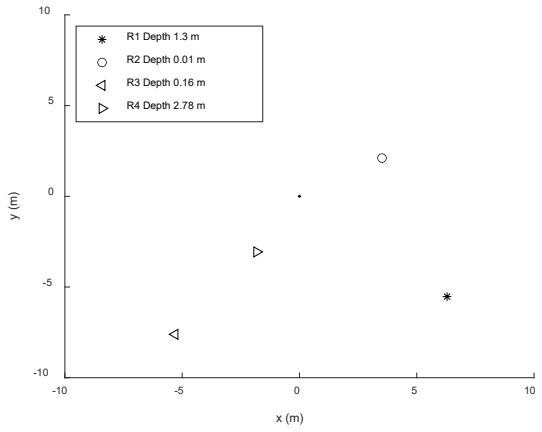

Figure 7: Optimised Receiver configuration

DISCUSSION

The mean localisation error of all receiver configurations, except run two, found by the PSO is 5.95 % smaller than the error of the original receiver configuration. The best solution is 6.64 % better than the original configuration. The optimal solution for the receiver configuration seems not to be a symmetric configuration (Figure 7). Figure 8 shows the receiver configuration of all successful optimisation runs. It can be observed from the figure that all solutions found by the PSO are not symmetric configurations.

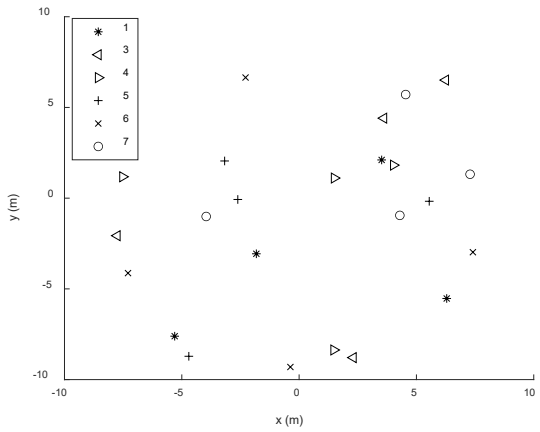

Figure 8: Receiver Configuration of all Successful Optimisation Runs

It can be observed from Figure 8 that in all configurations, except configuration 6, the receivers form a T-shaped baseline. Configuration six has the worst fitness value, compared to the other optimised solutions. The chosen penalty function does not allow the PSO to exploit any information from invalid receiver configurations. Therefore, if the whole population is outside the allowed area, the PSO is sometimes not able to find a suitable solution. Potentially, a penalty function, which takes the degree of violation into account when calculating the penalty value, might improve the performance of the optimisation.

CONCLUSION AND FUTURE WORK

The focus of this paper was an investigation of the localisation error using an SBL system. For this purpose, in a first step, different possible error influences are identified and a possible numerical simulation of the influence on the SBL was discussed. In the second step, the described simulation was used to determine the optimal position of the receivers of the system using PSO and Monte-Carlo simulations. For comparison, a standard configuration of the receivers, arranged in a symmetrical rectangular shaped baseline, was also simulated. The positioning error of the optimised receiver arrangement is 6.64 % smaller than the error of the standard arrangement. The accuracy specified by the manufacturer is one percent of the range, i.e. at a range of 100 m the accuracy is 1 m (Water Linked AS, 2020). The localisation error of the simulation is in the same order of magnitude as the proposed accuracy of the real SBL system used.

In future work the theoretical localisation error, calculated in this work, will be compared to real measured localisation errors. Furthermore, a cellular automaton (Tholen, et al., 2019) will be used in order to simulate the spatial and temporal changes in the speed of sound distribution and for the calculation of the hydrostatical pressure. In addition, other possible error sources, for example multi path propagation, will be

modelled and their impact on the localisation error will be analysed.

REFERENCES

Almeida, R., Melo, J. & Cruz, N., 2016. Characterization of measurement errors in a LBL positioning system. *IEEE OCEANS 2016 - Shanghai,*, pp. 1-6.

Bingham, B., 2009. Predicting the Navigation Performance of Underwater Vehicles. *The 2009 IEEE/RSJ International Conference on Intelligent Robots and Systems*, pp. 261-266.

Coello, C. A. C., 1999. *A survey of Constraint Handling Techniques used with Evolutionary Algorithms,* Avanzada: Lania-RI-99-04, Laboratorio Nacional de Informática Avanzada.

Eberhardt, R. & Shi, Y., 2000. Comparing Inertia Weights and Constriction Factors in Particle Swarm Optimization. *Proceedings of the 2000 Congress on Evolutionary Computation. CEC00*, pp. 84-88.

Kennedy, J. & Eberhart, R., 1995. Particle swarm optimization. *IEEE International Conference on: Neural Networks, Vol. 4*, pp. 1942-1948.

Nayar, K., Sharqawy, M. & Banchik L. D. Lienhard, J., 2016. Termophysical properties of seawater: A review and new correlations that include pressure dependence. *Desalination (390)*, pp. 1-24.

Nolle, L., 2015. On a search strategy for collaborating autonomous underwater vehicles. *Proceedings of Mendel 2015, 21st International Conference on Soft Computing*, pp. 159-164.

Parsopoulos, K. E. & Vrahatis, M. N., 2005. Unified Particle Swarm Optimization for Solving Constrained Engineering Optimization Problems. *Advances in Natural Computation. ICNC 2005. Lecture Notes in Computer Science, vol 3612*, pp. 582-591.

Paull, L., Saeedi, S., Seto, M. & Li, H., 2014. "AUV Navigation and Localization: A Review,". *IEEE Journal of Oceanic Engineering, vol. 39, no. 1*, pp. 131-149.

Tholen, C. et al., 2019. Automated Tuning Of A Cellular Automata Using Parallel Asynchronous Particle Swarm Optimisation. *Proceedings of the 33rd International ECMS Conference on Modelling and Simulation*, pp. 30-36.

Tholen, C., El-Mihoub, T., Nolle, L. & Zielinski, O., 2018. On the robustness of self-adaptive Levy-flight. *OCEANS - MTS/IEEE Kobe Techno-Oceans (OTO), Kobe*, pp. 1-5.

Tholen, C. & Nolle, L., 2017. Parameter Search for a small swarm of AUVs using Particle Swarm Optimisation. *Artificial Intelligence XXXIV. SGAI 2017. Lecture Notes in Computer Science, vol 10630*, pp. 384-396.

Tholen, C. et al., 2020. On the localisation of artificial submarine groundwater discharge sites using a low-cost multi-sensor-platform. *2020 OCEANS Singapore (to appear)*.

Turetta, A. et al., 2014. Analysis of the Accuracy of a LBL-based Underwater Localization Procedure. *IEEE Oceans - St. John's (Newfoundland)*, pp. 1-7.

UNESCO, 1983. Algorithms for computation of fundamental properties of seawater. *Unesco technical papers in marine sciences (44)*.

Water Linked AS, 2020. *Water Linked AS Underwater GPS.* [Online]
Available at: https://waterlinked.com/underwater-gps/

Wu, Y. et al., 2019. Survey of underwater robot positioning navigation. *Applied Ocean Research (90)*, pp. 101845,.

AUTHOR BIOGRAPHIES

CHRISTOPH THOLEN graduated from the Jade University of Applied Science in Wilhelmshaven, Germany, with a Master degree in Mechanical Engineering in 2015. Since 2016 he is a research fellow at the Jade University of Applied Science in a joint project of the Jade University of Applied Science and the Institute for Chemistry and Biology of the Marine Environment (ICBM), at the Carl von Ossietzky University of Oldenburg for the development of a low cost and intelligent environmental observatory.

TAREK A. EL-MIHOUB graduated with a BSc in computer engineering from University of Tripoli, Tripoli, Libya. He obtained his MSc in engineering multimedia and his PhD in computational intelligence from Nottingham Trent University in the UK. He was an assistant professor at the Department of Computer Engineering, University of Tripoli. He is currently a postdoctoral researcher with Jade University of Applied Science. His current research is in the fields of applied computational intelligence and autonomous underwater vehicles.

LARS NOLLE graduated from the University of Applied Science and Arts in Hanover, Germany, with a degree in Computer Science and Electronics. He obtained a PgD in Software and Systems Security and an MSc in Software Engineering from the University of Oxford as well as an MSc in Computing and a PhD in Applied Computational Intelligence from The Open University. He worked in the software industry before joining The Open University as a Research Fellow. He later became a Senior Lecturer in Computing at Nottingham Trent University and is now a Professor of Applied Computer Science at Jade University of Applied Sciences. His main research interests are computational optimisation methods for real-world scientific and engineering applications.

ROBIN ROFALLSKI graduated from Jade University of Applied Sciences in Oldenburg, Germany with a Master degree in Geodesy and Geoinformatics in 2016. Since 2016, he holds a research fellow position at the Institute of Applied Photogrammetry and Geoinformatics at Jade University. His research interests are in underwater photogrammetry, camera calibration and dynamic metrology.

OLIVER RALLE graduated from the Jade University of Applied Science with a Bachelor degree in Mechanical Engineering in 2019. Currently he is studying his Master degree in Mechanical Engineering at Jade University of Applied Sciences.